

# Dalton Transactions

Accepted Manuscript



This is an *Accepted Manuscript*, which has been through the Royal Society of Chemistry peer review process and has been accepted for publication.

*Accepted Manuscripts* are published online shortly after acceptance, before technical editing, formatting and proof reading. Using this free service, authors can make their results available to the community, in citable form, before we publish the edited article. We will replace this *Accepted Manuscript* with the edited and formatted *Advance Article* as soon as it is available.

You can find more information about *Accepted Manuscripts* in the [Information for Authors](#).

Please note that technical editing may introduce minor changes to the text and/or graphics, which may alter content. The journal's standard [Terms & Conditions](#) and the [Ethical guidelines](#) still apply. In no event shall the Royal Society of Chemistry be held responsible for any errors or omissions in this *Accepted Manuscript* or any consequences arising from the use of any information it contains.

## Pentanuclear [2.2] Spirocyclic Lanthanide (III) Complexes: Slow

### Magnetic Relaxation of the Dy<sup>III</sup> Analogue

*Sourav Biswas,<sup>a</sup> Sourav Das,<sup>a,b</sup> Jan van Leusen,<sup>c</sup> Paul Kögerler\*<sup>c</sup> and Vadapalli Chandrasekhar\*<sup>a,d</sup>*

<sup>a</sup> Department of Chemistry, Indian Institute of Technology Kanpur, Kanpur-208016, India.

<http://www.iitk.ac.in>

<sup>b</sup> Department of Emerging Materials Science, DGIST, Daegu 711-873, Korea

<sup>c</sup> Institut für Anorganische Chemie, RWTH Aachen University, D-52074 Aachen, Germany.

<http://www.ac.rwth-aachen.de>

<sup>d</sup> National Institute of Science Education and Research, Institute of Physics Campus,

Sachivalaya Marg, PO: Sainik School, Bhubaneswar - 751 005, India.

<http://www.niser.ac.in>

AUTHOR EMAIL ADDRESS: [vc@iitk.ac.in](mailto:vc@iitk.ac.in); [paul.koegerler@ac.rwth-aachen.de](mailto:paul.koegerler@ac.rwth-aachen.de)

**Abstract**

The reaction of  $\text{LnCl}_3 \cdot 6\text{H}_2\text{O}$  ( $\text{Ln} = \text{Dy}^{3+}$ ,  $\text{Tb}^{3+}$  and  $\text{Ho}^{3+}$ ) with the multisite coordinating ligand  $N'$ -(2-hydroxy-3-(hydroxymethyl)-5-methylbenzylidene)acetohydrazide ( $\text{LH}_3$ ) in the presence pivalic acid ( $\text{PivH}$ ) leads to the formation of three isostructural homometallic pentanuclear complexes,  $[\text{Dy}_5(\text{LH})_4(\eta^1\text{-Piv})(\eta^2\text{-Piv})_3(\mu_2\text{-}\eta^2\eta^1\text{Piv})_2(\text{H}_2\text{O})] \cdot \text{Cl} \cdot 9.5\text{H}_2\text{O} \cdot 5\text{MeOH}$  (1),  $[\text{Tb}_5(\text{LH})_4(\eta^1\text{-Piv})(\eta^2\text{-Piv})_3(\mu_2\text{-}\eta^2\eta^1\text{Piv})_2(\text{H}_2\text{O})] \cdot \text{Cl} \cdot 10.5\text{H}_2\text{O} \cdot 2\text{MeOH} \cdot 2\text{CHCl}_3$  (2) and  $[\text{Ho}_5(\text{LH})_4(\eta^1\text{-Piv})(\eta^2\text{-Piv})_3(\mu_2\text{-}\eta^2\eta^1\text{Piv})_2(\text{H}_2\text{O})] \cdot \text{Cl} \cdot 14.5\text{H}_2\text{O} \cdot 2\text{CHCl}_3$  (3). 1–3 are monocationic and are comprised of four doubly deprotonated  $[\text{LH}]^{2-}$  ligands along with six pivalate ions. These complexes possess a [2.2] spirocyclic topology formed by the fusion of two triangles of  $\text{Ln}^{\text{III}}$  ions at a common vertex. The magneto chemical analysis reveals the presence of antiferromagnetic exchange interactions at low temperature, and the  $\text{Dy}^{\text{III}}$  complex 1 gives an out-of-phase signal with a small curvature in alternating current (ac) magnetic susceptibility measurements. Application of a 3000 G static field during ac measurements intensifies the signals, revealing a second slow relaxation process in  $\text{Dy}^{\text{III}}$  analogue.

**Keywords:** pentanuclear lanthanide complexes, [2.2] spirocyclic complexes, single-molecule magnets, ac susceptibility, slow magnetic relaxation, Schiff base ligands.

## Introduction

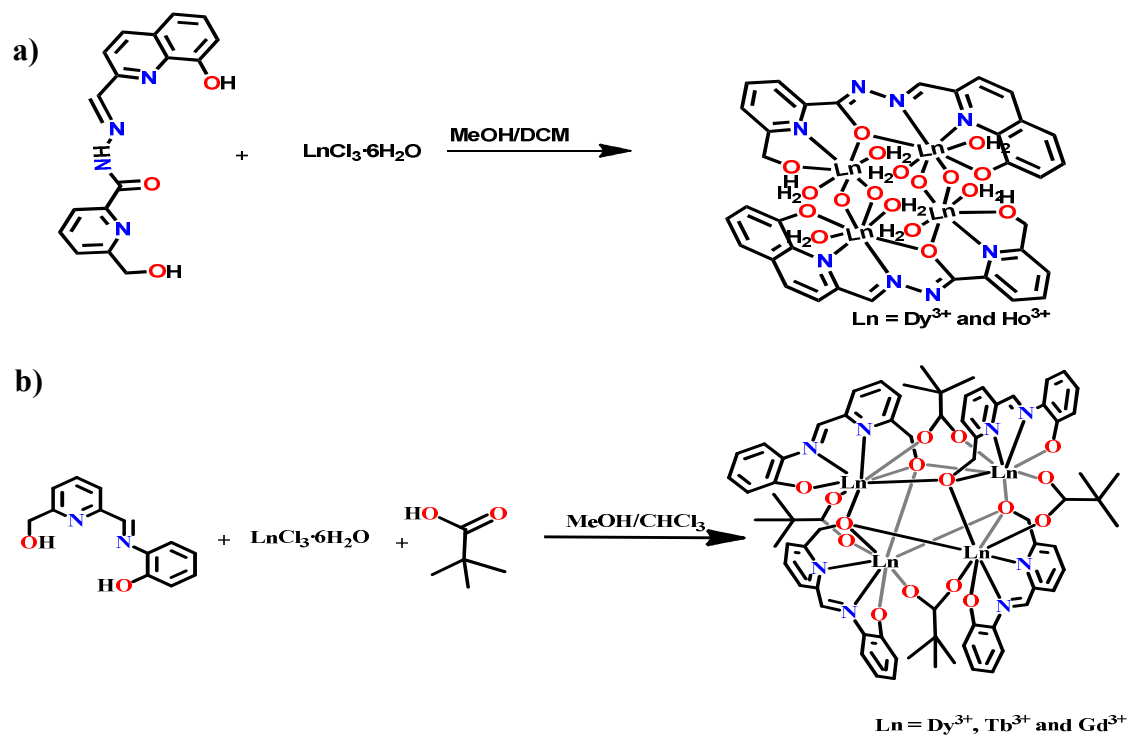
The synthesis of polynuclear clusters of 4f metal ions is of interest because of their potential utility in single-molecule magnets (SMMs), catalysis<sup>1</sup>, luminescence<sup>2</sup>, medical imaging<sup>3</sup>, magnetic refrigeration<sup>4</sup>, high-density data storage<sup>5</sup>, spintronics<sup>6</sup> and quantum computing<sup>7</sup>. SMMs are characterized by a slow relaxation of magnetization below the blocking temperature,  $T_B$ . Magnetic phenomena have been thoroughly explored in polynuclear 3d metal complexes<sup>8,9</sup> and heterometallic 3d/4f complexes<sup>10</sup>, and recent years have seen the emergence of lanthanide complexes, particularly those involving  $Dy^{3+}$  or  $Tb^{3+}$ . Here, the zero-field splitting of the  $m_J$  sub-states belonging to the  $J$  ground state produces the thermal energy barriers. Interest in lanthanide complex SMMs has been fueled by the seminal discovery by Winpenny and co-workers of complexes  $[Dy_4K_2O(O^iBu)_{12}]$  and  $[Dy_5O(O^iPr)_{13}]$ , possessing exceptionally high energy barriers for magnetization reversal.<sup>11</sup> Homometallic 4f complexes of varying nuclearities ( $Ln^{12}$ ,  $Ln_2^{13}$ ,  $Ln_3^{14}$ ,  $Ln_4^{15}$ ,  $Ln_5^{16}$ ,  $Ln_6^{17}$ ,  $Ln_7^{18}$ ,  $Ln_8^{19}$ ,  $Ln_9^{20}$ ,  $Ln_{10}^{21}$  and  $Ln_{11}^{22}$ ) are now documented in literature, and we have reported new SMMs involving 3d/4f<sup>23</sup> and 4f<sup>24</sup> metal ions. The five examples of pentanuclear lanthanide complexes known displaying three distinct structural topologies: pyramidal<sup>16a,16b,16c</sup>, butterfly<sup>16e</sup> and trigonal bipyramidal<sup>16d</sup>. These pentanuclear complexes evince SMM behavior including Winpenny's  $[Dy_5O(O^iPr)_{13}]$  complex, which showed a slow relaxation of magnetization with a  $528 \pm 11$  K thermal energy barrier<sup>16a</sup>. To pursue new polynuclear lanthanide complexes, we have designed a new linear alkyl hydrazone-based multidentate Schiff base ligand,  $N'$ -(2-hydroxy-3-(hydroxymethyl)-5-methylbenzylidene)acetohydrazide (LH<sub>3</sub>); upon reaction with  $LnCl_3 \cdot 6H_2O$  ( $Ln = Dy^{3+}$ ,  $Tb^{3+}$  and  $Ho^{3+}$ ), this afforded homometallic pentanuclear [2.2] spirocyclic complexes **1–3**,  $[Ln_5(LH)_4(\eta^1-Piv)(\eta^2-Piv)_3(\mu_2-\eta^2 \eta^1 Piv)_2(H_2O)] \cdot Cl \cdot xH_2O \cdot yMeOH \cdot zCHCl_3$  ( $Dy^{3+}$ ,  $x = 9.5$ ,  $y = 5$ ,  $z = 0$ ;  $Tb^{3+}$ ,  $x$

= 10.5,  $y = 2$ ,  $z = 2$  and  $\text{Ho}^{3+}$ ,  $x = 14.5$ ,  $y = 0$ ,  $z = 2$ ). In these complexes two triangles of  $\text{Ln}^{3+}$  ions are fused through a common vertex. The synthesis, structure and magnetic properties of these complexes are discussed herein.

## Results and Discussion

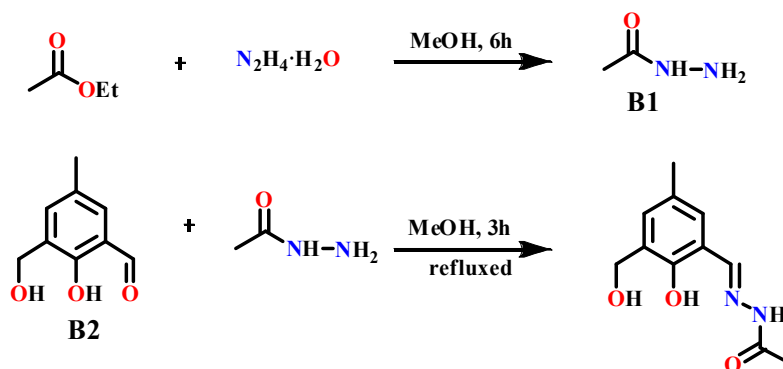
### Synthesis

Ligand design is a crucial element in modulating nuclearity and structural topology of lanthanide complexes. Recently, we have prepared rhombus-shaped  $\text{Ln}_4$  complexes,  $[\text{Ln}_4(\text{LH})_2(\mu_2\text{-O})_4(\text{H}_2\text{O})_8]$  ( $\text{Ln} = \text{Dy}^{3+}$  and  $\text{Ho}^{3+}$ ),<sup>25</sup> incorporating an aroyl hydrazone-based Schiff base ligand (6-hydroxymethyl)-*N'*-((8-hydroxyquinolin-2-yl)-methylene)picolinohydrazide (Scheme 1a).



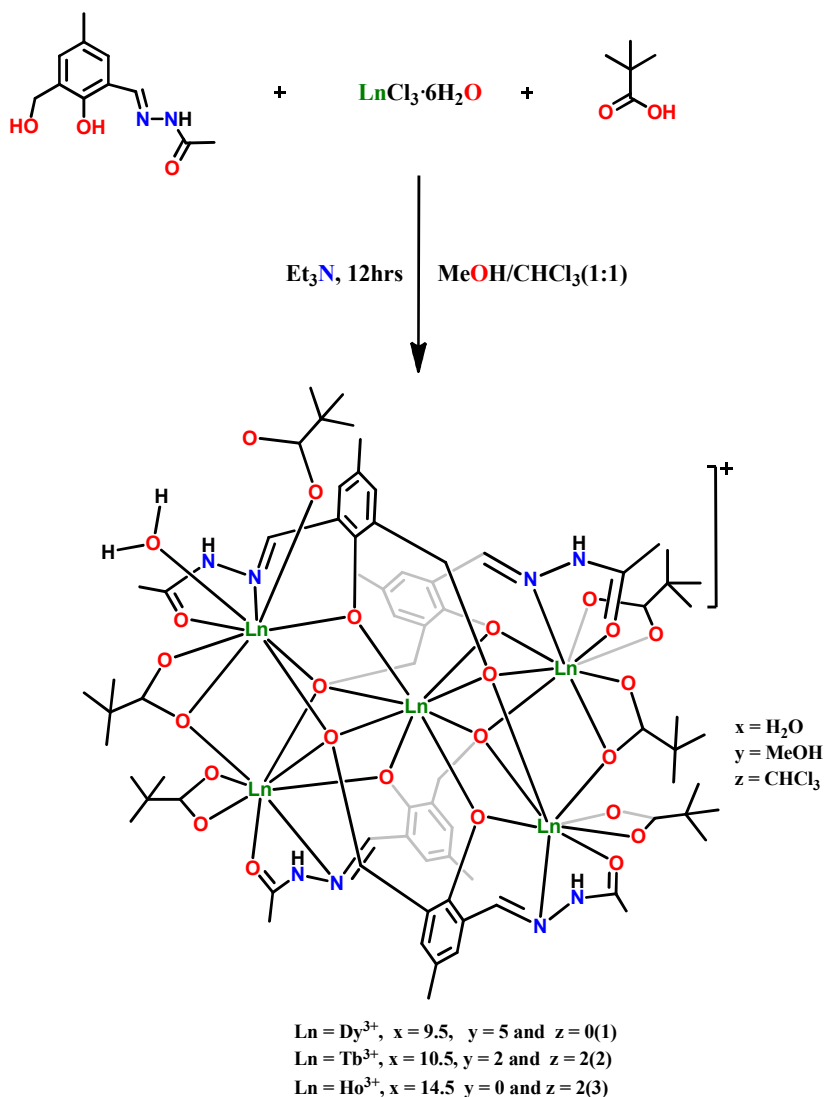
**Scheme 1.** a) Synthesis of rhombus-shaped tetranuclear lanthanide complexes<sup>25</sup> b) Synthesis of cubane-shaped tetranuclear lanthanide complexes<sup>27</sup>.

Motivated by this work, as well as by the use of other hydrazone-based Schiff base ligands in recent literature<sup>14c,15d,17d,24</sup>, we have prepared a multisite coordinating semi-flexible alkyl hydrazone-based ligand, *N*'-(2-hydroxy-3-(hydroxymethyl)-5-methylbenzylidene)acetohydrazide (LH<sub>3</sub>). This was produced using a two-step synthetic protocol that involved the preparation of B1, which subsequently undergoes a condensation reaction with B2 to give LH<sub>3</sub> (Scheme 2). The semi flexible ligand, LH<sub>3</sub> provides five divergent coordinating sites: an alkyl hydrazone oxygen, an imine N, an amide N, a phenolic O and a flexible –CH<sub>2</sub>OH arm. The latter is a crucial element to the formation of the coordination geometry, as recently shown by us in the preparation of cubane-shaped tetranuclear lanthanide complexes (Scheme 1b).<sup>27</sup> The pivalic acid co-ligands help to saturate the primary coordination spheres of the metals by bridging the metal centers, and confer lipophilicity to the complexes.



**Scheme 2.** Synthesis of the ligand LH<sub>3</sub>.

The reaction of LH<sub>3</sub>, LnCl<sub>3</sub>·6H<sub>2</sub>O, and pivalic acid in the stoichiometric ratio of 4:5:6 in the presence of 4 equivalents of triethylamine in methanol afforded pentanuclear Ln<sup>3+</sup> [Ln<sub>5</sub>(LH)<sub>4</sub>(η<sup>1</sup>-Piv)(η<sup>2</sup>-Piv)<sub>3</sub>(μ<sub>2</sub>-η<sup>2</sup> η<sup>1</sup>Piv)<sub>2</sub>(H<sub>2</sub>O)]·Cl·xH<sub>2</sub>O·yMeOH·zCHCl<sub>3</sub> [compound **1**, Ln = Dy<sup>3+</sup>, x = 9.5, y = 5, z = 0; compound **2**, Ln = Tb<sup>3+</sup>, x = 10.5, y = 2, z = 2 and compound **3**, Ln = Ho<sup>3+</sup>, x = 14.5, y = 0, z = 2] (Scheme 3).



**Scheme 3.** Synthesis of  $[\text{Ln}_5(\text{LH})_4(\eta^1\text{-Piv})(\eta^2\text{-Piv})_3(\mu_2\text{-}\eta^2\text{-}\eta^1\text{-Piv})_2(\text{H}_2\text{O})] \cdot \text{Cl} \cdot x\text{H}_2\text{O} \cdot y\text{MeOH} \cdot z\text{CHCl}_3$  ( $\text{Dy}$ ,  $x = 9.5$ ,  $y = 5$ ,  $z = 0$ ;  $\text{Tb}$ ,  $x = 10.5$ ,  $y = 2$ ,  $z = 2$  and  $\text{Ho}$ ,  $x = 14.5$ ,  $y = 0$ ,  $z = 2$ ).

### X-ray Crystal Structures

Single-crystal X-ray diffraction measurements reveal that compounds **1–3** are isostructural, and crystallize in the tetragonal space group  $I-4$  with  $Z = 4$ . The complexes are monocationic, with

their charges each balanced by a chloride anion, and possess a [2.2] spirocycle of Ln<sup>III</sup> ions containing two fused triangular motifs. Complex **1** has been chosen as a representative example to illustrate the common structural features of these clusters. Selected bond parameters of **1** are summarized in Table 1. The molecular structure and selected bond parameters of the other complexes (**2** and **3**) are presented in the ESI (Figures S1–S2 and Tables S1–S2). A perspective view of the molecular structure of **1** is depicted in Figure 1.

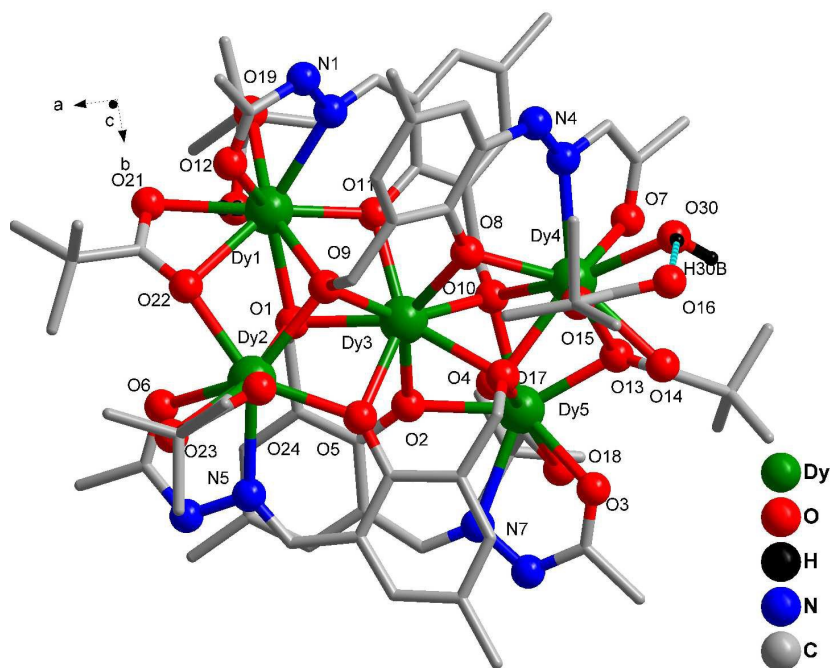


**Figure 1.** Molecular structure of **1** (selected hydrogen atoms, chloride and the solvent molecules have been omitted for clarity).



**Table 1.** Selected bond distances (Å) and bond angles (deg) parameters for **1**.

<b>Selected bond length around Dy1</b>	Dy(1)-O(11)	2.310(6)	Dy(3)-O(8)	2.321(6)	Dy(5)-O(4)	2.387(6)		
	Dy(1)-O(12)	2.396(7)	Dy(3)-O(9)	2.330(6)	Dy(5)-O(10)	2.409(6)		
	Dy(1)-O(20)	2.409(7)	Dy(3)-O(11)	2.351(6)	Dy(5)-O(18)	2.456(9)		
	Dy(1)-O(9)	2.417(6)	Dy(3)-O(4)	2.351(6)	Dy(5)-N(7)	2.508(9)		
	Dy(1)-O(19)	2.442(7)	Dy(3)-O(4)	2.351(6)	<b>Selected Bond angles around Dy</b>			
	Dy(1)-O(21)	2.447(6)	Dy(3)-O(1)	2.353(6)				
	Dy(1)-O(1)	2.457(6)	Dy(3)-O(2)	2.381(7)				
	Dy(1)-N(1)	2.519(8)	Dy(3)-O(5)	2.414(6)				
	Dy(1)-O(22)	2.521(6)	<b>Selected bond length around Dy4</b>					
	<b>Selected bond length around Dy2</b>	Dy(2)-O(24)		2.320(7)		Dy(4)-O(15)	2.312(7)	Dy(2)-O(1)-Dy(1)
Dy(2)-O(5)		2.324(6)		Dy(4)-O(8)		2.373(6)	Dy(3)-O(1)-Dy(1)	94.3(2)
Dy(2)-O(22)		2.325(6)		Dy(4)-O(7)		2.384(7)	Dy(5)-O(2)-Dy(3)	97.2(2)
Dy(2)-O(1)		2.333(6)		Dy(4)-O(4)		2.396(6)	Dy(3)-O(4)-Dy(5)	95.2(2)
Dy(2)-O(6)		2.402(7)		Dy(4)-O(30)		2.411(7)	Dy(3)-O(4)-Dy(4)	96.9(2)
Dy(2)-O(9)		2.439(6)		Dy(4)-N(4)	2.494(8)	Dy(5)-O(4)-Dy(4)	99.5(2)	
Dy(2)-N(5)		2.450(8)		Dy(4)-O(10)	2.500(6)	Dy(2)-O(5)-Dy(3)	95.3(2)	
Dy(2)-O(23)		2.454(7)		Dy(4)-O(14)	2.505(8)	Dy(3)-O(8)-Dy(4)	98.4(2)	
<b>Selected bond length around Dy3</b>		Dy(3)-O(10)		2.301(6)	Dy(4)-O(13)	2.666(9)	Dy(3)-O(9)-Dy(1)	95.9(2)
				<b>Selected bond length around Dy5</b>	Dy(5)-O(13)	2.258(7)	Dy(3)-O(9)-Dy(2)	94.5(2)
			Dy(5)-O(2)		2.286(6)	Dy(1)-O(9)-Dy(2)	96.18(9)	
			Dy(5)-O(17)		2.356(11)	Dy(3)-O(10)-Dy(5)	96.0(2)	
			Dy(5)-O(3)		2.381(7)	Dy(3)-O(10)-Dy(4)	95.4(2)	
					Dy(5)-O(10)-Dy(4)	96.1(2)		
				Dy(1)-O(11)-Dy(3)	98.3(2)			
				Dy(5)-O(13)-Dy(4)	95.4(3)			
				Dy(2)-O(22)-Dy(1)	96.4(2)			
				Dy(2)-O(1)-Dy(3)	96.7(2)			

The pentanuclear complex **1** is formed by the concerted coordination action of the four doubly deprotonated ligands [LH]<sup>2-</sup>. Four out of five potential coordinating sites of the ligand coordinated to the metal centers: a phenolate oxygen which functions as a bridging ligand between two Dy<sup>3+</sup> centers, a deprotonated hydroxymethyl arm which functions as a  $\mu_3$ -capping ligand among three Dy<sup>III</sup> centers, an imine nitrogen binding a Dy<sup>3+</sup> center, and an acetohydrazide

oxygen coordinating a Dy<sup>3+</sup> center. The framework provided by the ligand [LH]<sup>2-</sup> is bolstered by the coordination of six pivalate ligands: one is  $\eta^1$ -coordinated to Dy4, while three others chelate Dy1, Dy2 and Dy5 in  $\eta^2$  fashion. The remaining two pivalate ligands exhibit both bridging and chelating modes ( $\mu_2-\eta^2:\eta^1$ ) in their coordination that links Dy1 to Dy2 and Dy4 to Dy5. The pentanuclear [2.2] spirocyclic core is thus constructed by the coordination action of four [LH]<sup>2-</sup> ( $\mu_4-\eta^3:\eta^2:\eta^1:\eta^1$ ) and six pivalate ligands. The coordination modes of the ligands are depicted in Figure 2.

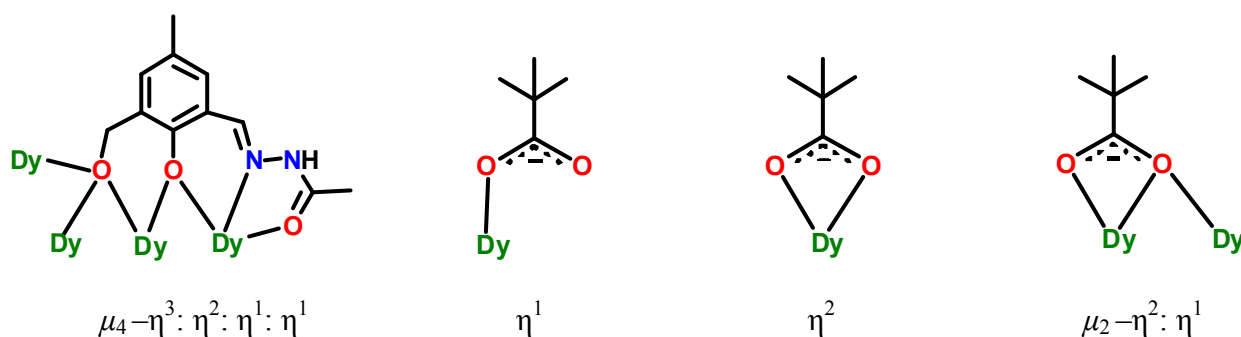


**Figure 2.** Binding modes of [LH]<sup>2-</sup> and the pivalate ligands with Dy<sup>3+</sup> ions in **1**.

The pentacationic pentanuclear core, [Dy<sub>5</sub>( $\mu_3$ -O)<sub>4</sub>( $\mu_2$ -O)<sub>4</sub>( $\mu_2$ - $\eta^2$ - $\eta^1$ -Piv)<sub>2</sub>]<sup>5+</sup> consists of two Dy<sub>3</sub> triangles which are interconnected by sharing a common vertex, Dy3. The remaining four vertices of the two triangles are occupied by Dy1, Dy2, Dy4 and Dy5 (Figure 3a). The edges of the triangles are formed by the pivalate ligands as well as phenolate oxygens of the ligand [LH]<sup>2-</sup> while the faces of the triangle are effectively capped by  $\mu_3$ -O, emanating from the flexible pendant hydroxymethyl arms (Figure 3a). The capping  $\mu_3$  oxygen atoms lie an average of ~1.219 Å away from the two triangular planes. The triangles are nearly equilateral, with Dy...Dy

vertex lengths of 3.50–3.651 Å and Dy–Dy–Dy angles that range from 58.1°– 62.2°. The two triangles are twisted at the Dy<sub>3</sub> [2.2] spirocyclic node by a dihedral angle 55.85° (Figure 3b).

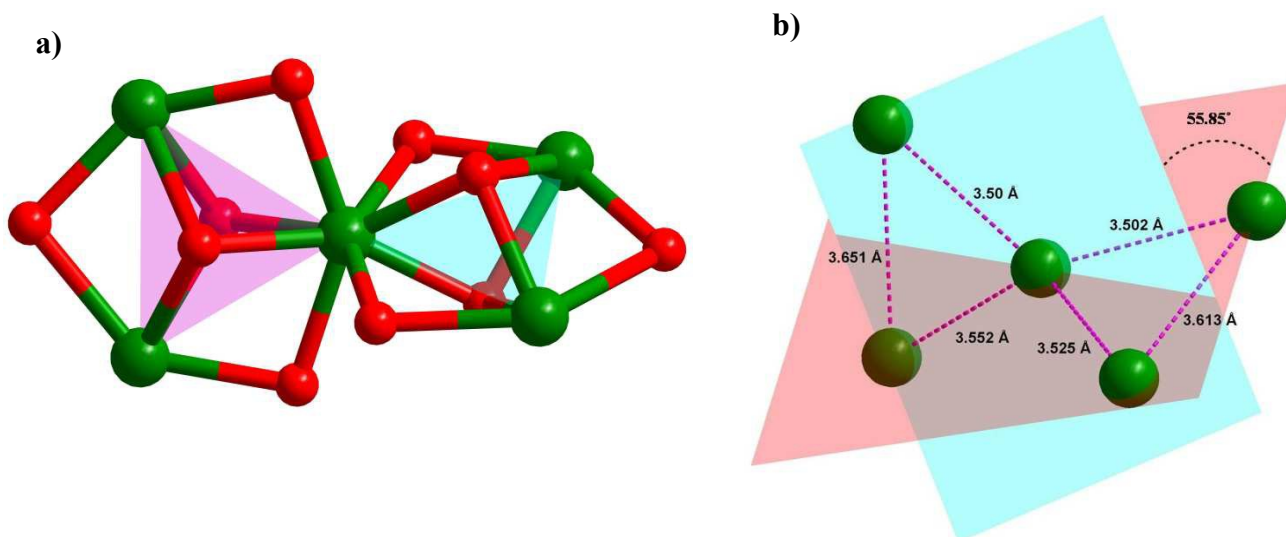


**Figure 3.** a) [2.2] spirocyclic core of the complex **1** b) [2.2] spirocyclic core showing the dihedral angle between the two triangular motifs along with the distance between the Dy<sup>3+</sup> centers.

The five crystallographically independent lanthanide centers present in **1** can be classified into three coordination geometry types (all distorted): triangular dodecahedron (Dy1, Dy5), square antiprism (Dy3), and mono-capped square-anti-prism (Dy2, Dy4) (Figure 4). A minor variation exists in the coordination environment around Dy2 and Dy4: unlike the rest of the dysprosium centers, Dy4 is coordinated by a water molecule, which is engaged in strong hydrogen bonding with the oxygen atom of the  $\eta^1$ -pivalate ligand (Figure 1) (D–H $\cdots$ A distance 1.746 Å and angle 154.41°) accounting for the  $\eta^1$  binding mode rather than the anticipated  $\eta^2$  coordination mode of the pivalate ligand. The Dy–O<sub>phenoxy</sub> bond lengths fall the range of ~2.286–2.414 Å which are slightly shorter than the Dy–O<sub>alkoxy</sub> bond lengths (~2.330–2.457 Å). These are in turn shorter

than many Dy–O<sub>piv</sub> bond distances that range from ~2.258 to ~2.660 Å. Bond lengths involving the coordinated imine nitrogens lie in the range of ~2.449–2.519 Å. The Dy–O<sub>phen</sub>–Dy (95.31°–98.36°) and Dy–O<sub>piv</sub>–Dy angles (95.36–96.36°) are in a similar range.

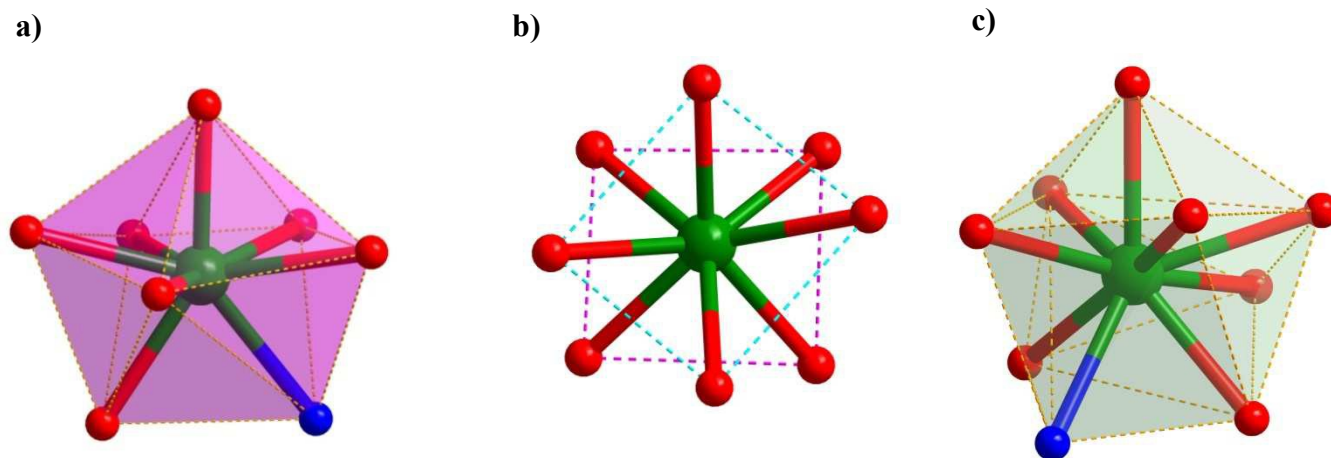


**Figure 4.** Local geometry around the three types of dysprosium centres in **1**: a) Dy1 and Dy5 possessing a distorted triangular dodecahedral geometry, b) Dy3 possessing a distorted square antiprism geometry and c) Dy2 and Dy4 possessing a distorted monocapped square antiprism.

The [2.2] spirocyclic topology observed in complexes **1-3** is quite distinct from the pyramidal<sup>16a,16b,16c</sup>, butterfly<sup>16e</sup> or trigonal bipyramidal<sup>16f</sup> shaped homometallic Ln<sub>5</sub> clusters reported previously (Figure S9). A comparison of the geometry around the metal centers, the structural topology around the metal ions and the SMM properties of the pentanuclear lanthanide families are summarized in Table 2.

**Table 2:** Structural and magnetic features of pentanuclear lanthanide assemblies.

Compound	Core topology	Coordination numbers (local geometries around Ln(III) centers)	Magnetic properties	References
$[\text{Dy}_5(\mu_3\text{-OH})_6(\text{Acc})_6(\text{H}_2\text{O})_{10}]\cdot\text{Cl}_9$ Acc = 1-amino cyclohexane-1-carboxylic acid.	Trigonal bipyramidal	Eight coordinated (distorted square-antiprism)	SMM $U_{\text{eff}} = 1.91 \text{ K}$ $\tau_0 = 1.01 \times 10^{-6} \text{ s}$	16d
$[\text{Dy}_5\text{O}(\text{O}^i\text{Pr})_{13}]$ $^i\text{Pr}$ = isopropyl	Square pyramidal	Six coordinated (octahedral)	SMM $U_{\text{eff}} = 528 \pm 11 \text{ K}$ , $46.6 \pm 0.7 \text{ K}$ $\tau_0 = 4.7 \times 10^{-10} \text{ s}$ , $3.8 \times 10^{-6} \text{ s}$	16a
$[\text{Dy}_5(\text{OH})_5(\alpha\text{-AA})_4(\text{Ph}_2\text{acac})_6]$ $\alpha\text{-AA}$ = D-PhGly	Square pyramidal	Eight coordinated	SMM	16b
$[\text{Dy}_5(\mu_3\text{-OH})_3(\text{opch})_6(\text{H}_2\text{O})_3]$ $\text{H}_2\text{opch}$ = o-vanillin pyrazine acylhydrazone	Butterfly	Eight coordinated (distorted dodecahedral), nine coordinated (distorted mono-capped square-antiprismatic) and nine coordinated (distorted triplecapped prismatic)	SMM $U_{\text{eff}} = 8.1 ; 37.9 \text{ K}$ $\tau_0 = 1.7 \times 10^{-5} \text{ s}$ ; $9.7 \times 10^{-8} \text{ s}$	16e
$[\text{Dy}_5(\mu_3\text{-OH})_3(\text{opch})_6(\text{H}_2\text{O})_3](\text{ClO}_4)_2$ $\text{H}_2\text{opch}$ = o-vanillin pyrazine acylhydrazone	Butterfly	Eight coordinated (distorted dodecahedral), nine coordinated (distorted mono-capped	SMM $U_{\text{eff}} = 197 \text{ K}$ ; $\tau_0 = 3.2 \times 10^{-9} \text{ s}$	16e

		square-antiprismatic) and nine coordinated (distorted triplecapped prismatic)		
$[\text{Dy}_5(\text{LH})_4(\eta^1\text{-Piv})(\eta^2\text{-Piv})_3(\mu_2\text{-}\eta^2\text{-Piv})_2(\text{H}_2\text{O})]\cdot\text{Cl}$	[2.2] spirocycle	Eight coordinated (distorted triangulardodecahedral), eight coordinated (distorted square-antiprism) and nine coordinated (monocapped-square-antiprism)	Slow relaxation	This work

### Thermogravimetric study of complex 1–3

Thermogravimetric analysis reveals that all the complexes **1–3** exhibit almost a similar decomposition pattern towards heat treatment involving a two-step weight loss process (Figures S10-S12). A small weight loss in the region of 60–120 °C was observed for all the complexes which is in part due to the loss of solvents of crystallization. In all the cases, some of the solvent molecules of crystallization are lost rapidly as the crystals are brought outside the mother liquor at room temperature. In the second step, above 300 °C, rapid weight loss of all the complexes was observed, confirming the decomposition of the complexes.

## Magnetic Studies

Direct current (dc) magnetic susceptibility data for **1–3** are presented as  $\chi_m T$  vs.  $T$  curves at  $B = 0.1$  Tesla, and molar magnetization  $M_m$  vs. applied field  $B$  diagrams at  $T = 2$  K in Figure 5. For the Dy<sup>III</sup> analogue **1**,  $\chi_m T$  reaches a value of  $64.9 \text{ cm}^3 \text{ K mol}^{-1}$  at 290 K which is slightly below the range  $65.1\text{--}70.3 \text{ cm}^3 \text{ K mol}^{-1}$  expected<sup>27a</sup> for five non-interacting Dy<sup>3+</sup> ( ${}^6H_{15/2}$ ,  $J = 15/2$ ,  $g_J = 4/3$ ) centers. The decrease of  $\chi_m T$  with lowering temperature is gradual down to  $\sim 100$  K, and then more precipitous (approximate slope). This behavior and the low value of  $\chi_m T$  at 290 K have their origin in the ligand field effect (i.e. depopulation of the  $m_J$  sublevels) and potential antiferromagnetic exchange interactions within the compound (note that the distinct deviation from a linear behavior in  $\chi_m T$  is already introduced at higher temperatures  $T \approx 200$  K). Analysis of the dc magnetic susceptibility data for **2** and **3** reveals a similar behavior, and the  $\chi_m T$  values at 290 K are also slightly lower than those expected for the respective number of non-interacting lanthanide centers. For **2**,  $\chi_m T$  reaches  $58.1 \text{ cm}^3 \text{ K mol}^{-1}$  at 290 K (expected<sup>27a</sup>  $58.2\text{--}60.1 \text{ cm}^3 \text{ K mol}^{-1}$  for five non-interacting Tb<sup>III</sup> ( ${}^7F_6$ ,  $J = 6$ ,  $g_J = 3/2$ ) centers); for **3**,  $\chi_m T$  is  $66.1 \text{ cm}^3 \text{ K mol}^{-1}$  at 290 K (expected<sup>27a</sup>  $66.3\text{--}69.0 \text{ cm}^3 \text{ K mol}^{-1}$  for five non-interacting Ho<sup>III</sup> ( ${}^5I_8$ ,  $J = 8$ ,  $g_J = 5/4$ ) centers).

At 2 K, the molar magnetizations  $M_m$  of **1–3** (Figure 5, inset) indicate saturation and thus hint roughly at the ground state of the Ln<sup>III</sup> centers in each compound expected due to ligand field effects on the spin-orbit ground term, since the weak exchange interactions of lanthanides at zero field are eliminated by the applied maximum fields: all of the extrapolated saturation values are roughly right in the center between the minimum magnetization of corresponding five non-interacting Ln<sup>III</sup> centers ( $5g_J m_{J,\min} N_A \mu_B$ ) and the maximum magnetization of such centers

( $5g_J N_A \mu_B$ ). This indicates that neither all  $\text{Ln}^{\text{III}}$  centers of a compound are characterized by a ground state of minimal  $m_{J,\text{min}}$  ( $\pm 1/2$  for **1**, 0 for **2**, **3**) nor of the maximum  $m_J = J$ .

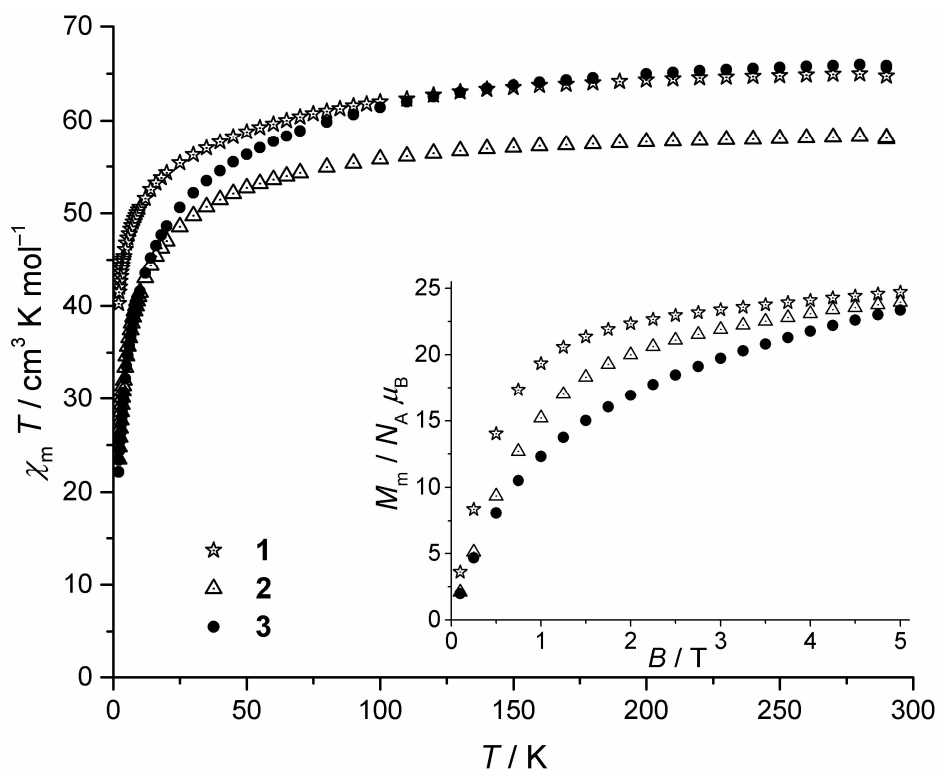


**Figure 5.** Temperature dependence of  $\chi_m T$  of **1–3** at 0.1 Tesla; inset: molar magnetization  $M_m$  as function of the applied field  $B$  at 2 K.

A comprehensive model of compounds **1–3** based exclusively on the magnetic susceptibility data is not feasible because the description of the compounds should include at least two different lanthanide sites (approximately  $D_{4d}$  and  $D_{3h}$  symmetric, eight- or nine-fold coordinated centers) and three different exchange pathways. Without a simpler model system such as  $\{\text{Gd}_5\}$ , or complementary data such as from inelastic neutron scattering, degenerate preliminary solutions modeled by the computational framework CONDON 2.0<sup>27b,27c</sup> cannot be ruled out. One feature common among all of these preliminary solutions provides qualitative insight into  $\chi_m T$  and  $M_m$  behavior presented in Figure 5: all calculations reveal very weak ferromagnetic exchange



interactions between the two outer lanthanides of each triangle (i.e. Ln1...Ln2 and Ln4...Ln5, Figure 3b), and either antiferromagnetic ( $\approx -0.3 \text{ cm}^{-1}$ ) or almost nonexistent exchange interactions for the remaining pathways (Ln1...Ln3, Ln2...Ln3, Ln3...Ln4, and Ln3...Ln5). Note that although the bridging ligands are similar, and thus exchange interactions might be assumed to be similar as well, the various distances between the Ln pairs and the presence of three different site geometries, and thus ligand fields, explain the difference in the exchange interaction parameters.

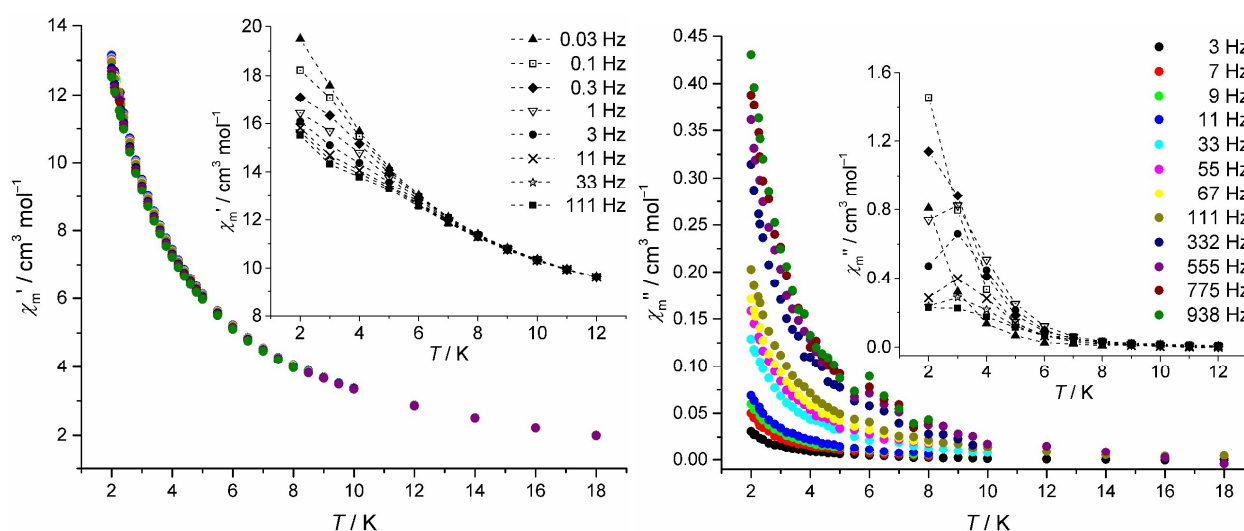


**Figure 6.** Left: in-phase magnetic susceptibility  $\chi_m'$  vs.  $T$ ; right: out-of-phase magnetic susceptibility  $\chi_m''$  vs.  $T$  of **1** at different frequencies  $f$  at zero dc bias field; insets: at 3000 G dc bias field (dashed lines are guides for the eye).

Alternating current (ac) molar magnetic susceptibility measurements on complexes **1–3** revealed out-of-phase signals for Dy<sup>III</sup> analogue **1**, but not for **2** and **3**, at zero dc field. The very small curvatures within the Argand plane for complex **1** (Figure S3) reveal in-phase signals  $\chi_m'$  that are almost independent from the applied frequency (Figure 6). The application of external static fields of up to 4000 G slightly shifted  $\chi_m'$ , but did not produce significantly greater curvatures for

frequencies greater than 100 Hz. Similar behavior was observed by Thielemann *et al.*<sup>16b</sup> who ascribed it to a blocking temperature which lies significantly below the range explored by the magnetic measurements. Optimal slow relaxation magnetic measurements of complex **1** with respect to the experimental options at hand were obtained using a 3000 G static field, and a frequency range of 0.03 Hz–111 Hz (Figure 7, insets Figure 6). The in-phase ( $\chi_m'$ ) and out-of-phase ( $\chi_m''$ ) ac susceptibility components can be fitted to a Cole-Cole equation<sup>28</sup> for each temperature (Figure 7, solid lines; Figure S3). To determine the average relaxation times of the magnetization under the optimized conditions, the temperature-dependent fit parameters have been analyzed using an Arrhenius expression ( $\tau = \tau_0 \cdot \exp(\Delta U/k_B T)$ ). This results in an effective energy barrier  $\Delta U = (5.2 \pm 0.5) \text{ cm}^{-1}$  and a time constant of  $\tau_0 = (2.6 \pm 0.6) \times 10^{-2} \text{ s}$  (Figure S5). In the generalized Debye model, the distribution width of  $\tau$  is parametrized by the scalar  $\alpha$ . The nonzero mean value of  $\alpha = 0.45 \pm 0.08$  reveals that several relaxation processes are active in this system. The time constant  $\tau_0$  is anomalously large for SMM behavior, i.e. the entirely phenomenological parameter  $\tau_0$  does not fall within the typical SMM range, and indicates that rather a secondary relaxation process was observed in the presence of a bias field instead of the relaxation process indicated at zero field. This is supported by the occurrence of the minima in the Cole-Cole curves for higher frequencies (lower  $\chi_m'$  values) hinting at further subsequent semi-circles which we could not enhance with the experimental set-up at hand. Since some or all exchange interactions within lanthanide compounds are overridden by the application of an external field of 3000 G, the observed process may be connected to a forced alignment of the momenta albeit further evidence is needed to proof this hypothesis.

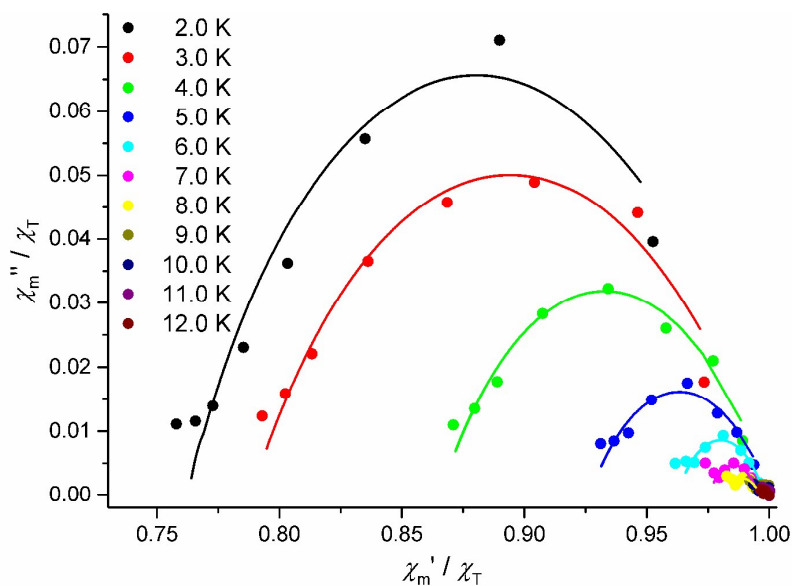


**Figure 7.** Normalized Cole-Cole plot of **1** at different temperatures and 3000 G dc field (solid circles), frequencies range from 0.03–111 Hz,  $\chi_T$  is the isothermal susceptibility in the limit of lowest frequencies; fit to Cole-Cole equation (solid lines).

## Conclusions

In summary, a series of isostructural homometallic pentanuclear  $\text{Ln}_5$  complexes that possess an unprecedented [2.2] spirocyclic topology were synthesized. The frameworks of these complexes are comprised of the multidentate Schiff base ligand, *N*-(2-hydroxy-3-(hydroxymethyl)-5-methylbenzylidene)acetohydrazide, along with several bridging pivalate groups. The lanthanide centers present in the pentanuclear assembly can be grouped into three types based on their local coordination geometry: an eight-coordinate lanthanide in a distorted triangular dodecahedral geometry, an eight-coordinate lanthanide in a distorted square-antiprism geometry and a nine-coordinate lanthanide in a mono-capped square anti-prism geometry. Variable-temperature dc and ac magnetic susceptibility measurements reveal weak antiferromagnetic exchange interactions among the lanthanide centers of complexes **1-3**. Compound **1** exhibited temperature-

dependent out-of-phase ac molar magnetic susceptibility signals with small curvatures at zero dc field. The application of a static 3000 G field intensified the ac magnetic susceptibility component, and an Arrhenius analysis confirmed slow magnetic relaxation of the Dy<sup>III</sup> analogue.

### Experimental Section

Solvents and other general reagents used in this work were purified according to standard procedures.<sup>29</sup> 2,6-Bis(hydroxymethyl)-4-methylphenol, activated manganese (IV) dioxide (MnO<sub>2</sub>), DyCl<sub>3</sub>·6H<sub>2</sub>O, TbCl<sub>3</sub>·6H<sub>2</sub>O and HoCl<sub>3</sub>·6H<sub>2</sub>O were obtained from Sigma Aldrich Chemical Co. and were used as received. Acetyl hydrazide and 2-(hydroxymethyl)-6-carbaldehyde-4-methylphenol were prepared according to the literature procedure<sup>23e</sup>. Hydrazine hydrate (80%), pivalic acid and sodium sulphate (anhydrous) were obtained from S.D. Fine Chemicals, Mumbai, India and were used as such.

**Instrumentation.** Melting points were measured using a JSGW melting point apparatus and are uncorrected. IR spectra were recorded as KBr pellets on a Bruker Vector 22 FT IR spectrophotometer operating at 400–4000 cm<sup>-1</sup>. Elemental analyses of the compounds were obtained from Thermoquest CE instruments CHNS-O, EA/110 model. <sup>1</sup>H NMR spectra were recorded in CD<sub>3</sub>OD solutions on a JEOL JNM LAMBDA 400 model spectrometer operating at 500.0 MHz, Chemical shifts are reported in parts per million (ppm) and are referenced with respect to internal tetramethylsilane (<sup>1</sup>H). Powder X-ray diffraction (PXRD) patterns were recorded with a Bruker D8 advance diffractometer equipped with nickel-filtered Cu K $\alpha$  radiation. Powder X-ray diffraction (PXRD) patterns of complexes **1–5** were in good agreement

with the simulated patterns (ESI, Figures S6–S8). The difference in intensities could be due to the preferred orientation in the powder samples.

**Magnetic Measurements.** Magnetic susceptibility data of **1–3** were recorded using a Quantum Design MPMS-5XL SQUID magnetometer for static field (DC) and dynamic field (AC) measurements. The polycrystalline samples were compacted and immobilized into PTFE capsules. DC susceptibility data were acquired as a function of the field (0.1–5.0 T) and temperature (2–290 K). AC susceptibility data were measured at zero field and in presence of various static fields in the frequency range 0.03–1000 Hz ( $T = 1.8–50$  K,  $B_{ac} = 3$  G,  $B_{dc} = 0–4000$  G). All data were corrected for the contribution of the sample holder (PTFE capsule) and the diamagnetic contributions of compound **1–3** calculated from tabulated values ( $-1.25 \times 10^{-3}$  cm<sup>3</sup> mol<sup>-1</sup>,  $-1.37 \times 10^{-3}$  cm<sup>3</sup> mol<sup>-1</sup> and  $-1.32 \times 10^{-3}$  cm<sup>3</sup> mol<sup>-1</sup>, respectively).

**X-ray Crystallography.** The crystal data for the compounds have been collected on a Bruker SMART CCD diffractometer (MoK $\alpha$  radiation,  $\lambda = 0.71073$  Å). The program SMART<sup>30a</sup> was used for collecting frames of data, indexing reflections, and determining lattice parameters, SAINT<sup>30a</sup> for integration of the intensity of reflections and scaling, SADABS<sup>30b</sup> for absorption correction, and SHELXTL<sup>30c,30d</sup> for space group and structure determination and least-squares refinements on  $F^2$ . All the structures were solved by direct methods using the program SHELXS-97<sup>30e</sup> and refined by full-matrix least-squares methods against  $F^2$  with SHELXL-97<sup>30e</sup>. Hydrogen atoms were fixed at calculated positions and their positions were refined by a riding model. All the non-hydrogen atoms were refined with anisotropic displacement parameters. The lattice solvent molecules of the complexes **1–3** cannot be modeled satisfactorily due to the presence of

very high disorder. PLATON/SQUEEZE<sup>30f,30g</sup> routine was utilized to remove those severely disordered solvents molecules. The total electron count thus squeezed is 396, 646 and 780 respectively per unit cell which corresponds to 99, 161 and 195 electrons per molecule ( $Z = 4$ ). These electron counts can be assigned to 5MeOH, H<sub>2</sub>O (expected 100) for **1**, 2CHCl<sub>3</sub>, 2MeOH, H<sub>2</sub>O (expected 162) for **2** and 2CHCl<sub>3</sub>, 8H<sub>2</sub>O (expected 196) for **3**. The crystallographic figures have been generated using Diamond 3.1e software<sup>30h</sup>. The crystal data and the cell parameters for compounds **1-3** are summarized in Table 3. Crystallographic data (excluding structure factors) for the structures in this paper have been deposited with the Cambridge Crystallographic Data Centre as supplementary publication nos. CCDC 1031235–1031237. Copies of the data can be obtained, free of charge, on application to CCDC, 12 Union Road, Cambridge CB2 1EZ, U.K.: <http://www.ccdc.cam.ac.uk/cgi-bin/catreq.cgi> , e-mail: [data\\_request@ccdc.cam.ac.uk](mailto:data_request@ccdc.cam.ac.uk), or fax: +44 1223 336033.

**Table 3.** Crystal data and structure refinement parameters of **1-3**.

	<b>1</b>	<b>2</b>	<b>3</b>
formula	C <sub>148</sub> H <sub>208</sub> Cl <sub>2</sub> Dy <sub>10</sub> N <sub>16</sub> O <sub>67</sub>	C <sub>148</sub> H <sub>206</sub> Cl <sub>2</sub> N <sub>16</sub> O <sub>69</sub> Tb <sub>10</sub>	C <sub>148</sub> H <sub>208</sub> Cl <sub>2</sub> Ho <sub>10</sub> N <sub>16</sub> O <sub>63</sub>
M/g	4979.22	4967.45	4939.52
crystal system	Tetragonal	Tetragonal	Tetragonal
space group	<i>I</i> -4	<i>I</i> -4	<i>I</i> -4
<i>a</i> /Å	40.368(2)	40.479(5)	40.446(5)
<i>b</i> /Å	40.368(2)	40.479(5)	40.446(5)
<i>c</i> /Å	11.922(7)	11.943(5)	11.940(5)
$\alpha=\beta=\gamma$ (°)	90	90	90
<i>V</i> /Å <sup>3</sup>	19429(2)	19569(10)	19532(9)
<i>Z</i>	4	4	4
$\rho$ /g cm <sup>-3</sup>	1.702	1.688	1.680
$\mu$ /mm <sup>-1</sup>	3.905	3.674	4.107
<i>F</i> (000)	9752.0	9768.0	9664.0
cryst size (mm <sup>3</sup> )	0.09 × 0.078 × 0.023	0.12 × 0.07 × 0.06	0.15 × 0.11 × 0.06

$\theta$ range (deg)	2.26 to 26.80	2.25 to 28.04	2.25 to 20.39
limiting indices	-43 $\leq$ h $\leq$ 51 -44 $\leq$ k $\leq$ 51 -15 $\leq$ l $\leq$ 14	-51 $\leq$ h $\leq$ 50 -51 $\leq$ k $\leq$ 51 -15 $\leq$ l $\leq$ 12	-49 $\leq$ h $\leq$ 29 -48 $\leq$ k $\leq$ 49 14 $\leq$ l $\leq$ 14
reflns collected	76684	68807	53438
ind reflns	21174 [R(int) =0.0722]	21266 [R(int) =0.1230]	18181[R(int) =0.0923]
completeness to $\theta$ (%)	99.9	99.8	100.0
refinement method	Full-matrix least-squares on $F^2$	Full-matrix least-squares on $F^2$	Full-matrix least-squares on $F^2$
data/restraints/params	21174 / 1 / 1068	21266 / 22 / 1101	18181 / 1 / 1081
goodness-of-fit on $F^2$	1.029	1.028	1.027
Final R indices [ $I > 2\theta(I)$ ]	$R_1 = 0.0501$ $wR_2 = 0.1065$	$R_1 = 0.0565$ $wR_2 = 0.1359$	$R_1 = 0.0676$ $wR_2 = 0.1536$
R indices (all data)	$R_1 = 0.0671$ $wR_2 = 0.1123$	$R_1 = 0.0828$ $wR_2 = 0.1532$	$R_1 = 0.1009$ $wR_2 = 0.1799$

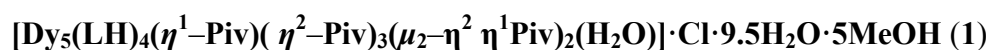
## Synthesis

### *N'*-(2-hydroxy-3-(hydroxymethyl)-5-methylbenzylidene)acetohydrazide (LH<sub>3</sub>)

To a stirred solution of 2-(hydroxymethyl)-6-carbaldehyde-4-methylphenol (1.50 g, 9.02 mmol) (**B2**) in 40 mL ethanol, acetyl hydrazide (0.66 g, 9.02 mmol) (**B1**) was added drop wise over a period of 15 minutes and the resultant yellow colored solution was refluxed for 5 hrs. Then, the yellow solution was concentrated in vacuo to 15 mL and kept in a refrigerator at 0 °C for overnight. A light yellow colored heavy precipitate was obtained which was filtered and washed with cold ethanol as well as diethyl ether before being dried. Yield: 1.6 g (79.8 %). Mp: 180 °C. FT-IR (KBr)  $\text{cm}^{-1}$ : 3398  $\nu(\text{O-H})$ ; 3181  $\nu(\text{N-H})$ ; 1661  $\nu(\text{C=O})$ ; 1624  $\nu(\text{C=N})_{\text{imine}}$ ; 1516  $\nu(\text{C=N})_{\text{py}}$ .  $^1\text{H NMR}$  ( $\text{CD}_3\text{OD}$ ,  $\delta$ , ppm, 500MHz ): 2.05 (s, 3H,  $-\text{CH}_3_{\text{acetyl}}$ ), 2.27 (s, 3H,  $-\text{CH}_3$ ), 4.55 (s, 2H,  $-\text{CH}_2\text{OH}$ ), 5.46 (s, 1H,  $-\text{OH}_{\text{phen}}$ ), 7.02 (s, 1H, Ar-H), 7.22 (s, 1H, Ar-H), 8.06 (s, 1H,  $-\text{NH}$ ), 8.17 (s, 1H, imine). Anal. Calcd for  $\text{C}_{11}\text{H}_{14}\text{N}_2\text{O}_3$ : C, 59.45; H, 6.35; N, 12.60 Found: C, 58.77; H, 6.01; N, 12.19. ESI-MS,  $m/z$ : (M+H)<sup>+</sup>. 223.09.

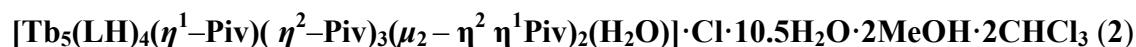
### General Synthetic Procedure for the Preparation of the Complexes 1–3.

All the pentanuclear complexes (1–3) have been synthesized according to the following procedure. LH<sub>3</sub> (0.04 g, 0.18 mmol) was dissolved in 40 mL methanol. To this solution, under stirring, LnCl<sub>3</sub>·6H<sub>2</sub>O (0.23 mmol) was added and the reaction mixture was stirred for 20 minutes at room temperature. At this stage, triethylamine (0.096 mL, 0.73 mmol) was added drop wise and the stirring was continued for a further 10 minutes and pivalic acid (0.028 g, 0.27 mmol) was added drop wise to the mixture. The resulting yellow colored solution was continued to stir for 12 hours at room temperature. Then, the solution was completely evaporated in vacuo to afford a light yellow colored solid mass which was washed 2–3 times with diethyl ether and dried. The solid mass was re-dissolved in MeOH/CHCl<sub>3</sub> (1:1) and kept for crystallization. After about 12 days, needle-shaped yellow colored crystals suitable for X-ray crystallography were obtained by slow evaporation from the solvent mixture. Specific details of each reaction and the characterization data of the products obtained are given below.

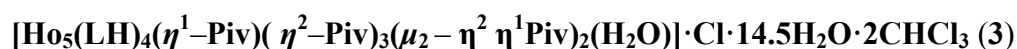


Quantities: LH<sub>3</sub> (0.04 g, 0.18 mmol), DyCl<sub>3</sub>·6H<sub>2</sub>O (0.087 g, 0.23 mmol), Et<sub>3</sub>N (0.096 mL, 0.73 mmol), PivH (0.028 g, 0.27 mmol). Yield: 0.076 g, 63.3 % (based on Dy<sup>3+</sup>). Mp: 200 °C (d). IR (KBr) (cm<sup>-1</sup>): 3433 (b), 2978 (s), 2950 (s), 2604 (s), 2497(s), 2343 (w), 1620 (s), 1574 (s), 1482 (s), 1429 (s), 1397 (s), 1309 (w), 1262 (w), 1228 (w), 1172 (w), 1072 (w), 1037 (s), 897 (w), 851 (w), 808 (s), 608 (w). Anal. Calcd. for C<sub>79</sub>H<sub>122</sub>Cl Dy<sub>5</sub> N<sub>8</sub> O<sub>39.5</sub> (2663.80): C, 35.62; H, 4.62 N, 4.21. Found: C, 34.96; H, 4.33 N, 4.09.





Quantities: LH<sub>3</sub> (0.04 g, 0.18 mmol), TbCl<sub>3</sub>·6H<sub>2</sub>O (0.085 g, 0.23 mmol), Et<sub>3</sub>N (0.096 mL, 0.73 mmol), PivH (0.028 g, 0.27 mmol). Yield: 0.058 g, 46.03 % (based on Tb<sup>3+</sup>). Mp: 200 °C (d). IR (KBr) (cm<sup>-1</sup>): 3441 (b), 2971 (s), 2930 (s), 2601 (s), 2499(s), 2339 (w), 1610 (s), 1570 (s), 1477(s), 1425 (s), 1393 (s), 1302 (w), 1252 (w), 1235 (w), 1178 (w), 1071 (w), 1032 (s), 895 (w), 854 (w), 803 (s), 610 (w). Anal. Calcd. for C<sub>78</sub>H<sub>112</sub>Cl<sub>7</sub>N<sub>8</sub>O<sub>37.5</sub>Tb<sub>5</sub> (2804.55): C, 33.40; H, 4.03; N, 4.00. Found: C, 32.93; H, 4.10 N, 4.04



Quantities: LH<sub>3</sub> (0.04 g, 0.18 mmol), HoCl<sub>3</sub>·6H<sub>2</sub>O (0.087 g, 0.23 mmol), Et<sub>3</sub>N (0.096 mL, 0.73 mmol), PivH (0.028 g, 0.27 mmol). Yield: 0.062 g, 48.4 % (based on Ho<sup>3+</sup>). Mp: 200 °C (d). IR (KBr) (cm<sup>-1</sup>): 3447 (b), 2965 (s), 2933 (s), 2607 (s), 2497(s), 2331 (w), 1603 (s), 1579 (s), 1475(s), 1424 (s), 1390 (s), 1297 (w), 1251 (w), 1233 (w), 1172 (w), 1070 (w), 1029 (s), 899 (w), 844 (w), 798 (s), 611 (w). Anal. Calcd. for C<sub>76</sub>H<sub>118</sub>Cl<sub>7</sub>Ho<sub>5</sub>N<sub>8</sub>O<sub>39.5</sub> (2848.60): C, 32.04; H, 4.18; N, 3.93. Found: C, 31.73; H, 4.23; N, 3.61.

**Electronic Supplementary Information (ESI):** Molecular structure of **2**, **3** (Figures S1-S2), list of bond length and bond angles (Tables S1-S2), Cole-Cole plot at zero dc field (Figure S3),  $\chi_m'$  vs.  $T$  plot at 3000 G (Figure S4),  $\chi_m''$  vs.  $T$  at 3000 G (Figure S5),  $\tau$  vs.  $T^{-1}$  (Figure S6) PXRD (Figure S6-S8), reported Ln5 complexes (Figure S9) and TGA (Figure S10-S12).

**Acknowledgements:** We thank the Department of Science and Technology (DST), India, for financial support, including support for a Single Crystal CCD X-ray Diffractometer facility at

IIT-Kanpur. V.C. is grateful to the DST for a J. C. Bose fellowship. S.B. thanks Council of Scientific and Industrial Research, India for Senior Research Fellowship.

### References:

1. (a) P. W. Roesky, G. C. Melchor and A. Zulys, *Chem. Commun.*, 2004, 738; (b) P. W. Roesky and T. E. Muller, *Angew. Chem. Int. Ed.*, 2003, **42**, 2708; (c) T. N. Parac-Vogt, K. Deleersnyder and K. Binnemans, *Eur. J. Org. Chem.*, 2005, 1810; (d) F. Pohlki, S. Doye, *Chem. Soc. Rev.*, 2003, **32**, 104; (e) X. Yu, S.Y. Seo and M. J. Tobin, *J. Am. Chem. Soc.*, 2007, **129**, 7244.
2. (a) M. Romanelli, G. A. Kumar, T. J. Emge, R. E. Riman and J. G. Brennan, *Angew. Chem., Int. Ed.*, 2008, **47**, 6049; (b) C. M. G. dos Santos, A. J. Harte, S. J. Quinn and T. Gunnlaugsson, *Coord. Chem. Rev.*, 2008, **252**, 2512; (c) S. L. Faulkner, S. Natrajan and D. Sykes, *Dalton Trans.*, 2009, 3890; (d) K. Binnemans, *Coord. Chem. Rev.*, 2009, **109**, 4283; (e) M. D. Ward, *Coord. Chem. Rev.*, 2007, **251**, 1663; (f) S. Sivakumar and M. L. P. Reddy, *J. Mater. Chem.*, 2012, **22**, 10852.
3. (a) A. Picot, A. D'Ale', P. L. Baldeck, A. Grichine, A. Duperray, C. Andraud and O. Maury, *J. Am. Chem. Soc.*, 2008, **130**, 1532; (b) M. Bottrill, L. Kwok and N. Long, *J. Chem Soc. Rev.*, 2006, **35**, 557.
4. (a) S. Biswas, H. S. Jena, A. Adhikary and S. Konar, *Inorg. Chem.* 2014, **53**, 3926; (b) S. Goswami, A. Adhikary, H. S. Jena and S. Konar, *Dalton Trans.*, 2013, **42**, 9813; (c) J. A. Sheikh, A. Adhikary and S. Konar, *New J. Chem.*, 2014, **38**, 3006; (d) L. Bogani and W. Wernsdorfer, *Nature Materials*, 2008, **7**, 179; (e) Y.-Z. Zheng, M. Evangelisti and R. E. P. Winpenny, *Angew. Chem., Int. Ed.*, 2011, **50**, 3692; (f) Y.-Z. Zheng, M. Evangelisti, F. Tuna and R. E. P. Winpenny, *J. Am. Chem. Soc.*, 2012, **134**, 1057; (g) Y.-Z. Zheng, M. Evangelisti and R.

E. P. Winpenny, *Chem. Sci.*, 2011, **2**, 99; (h) J. M. Jia, S. J. Liu, Y. Cui, S. D. Han, T.-L. Hu, and X. H. Bu, *Cryst. Growth Des.*, 2013, **13**, 4631.

5. (a) M. Affronte, *J. Mater. Chem.* **2009**, **19**, 1731; (b) A. R. Rocha, V. García-Suárez, S. W. Bailey, C. J. Lambert, J. Ferrerand and S. Sanvito, *Nat. Mater.*, 2005, **4**, 335; (c) M. Urdampilleta, S. Klyatskaya, J.-P. Cleuziou, M. Ruben and W. Wernsdorfer, *Nat. Mater.*, 2011, **10**, 502.

6. (a) J. D. Rinehart, M. Fang, W. J. Evans and J. R. Long, *J. Am. Chem. Soc.*, 2011, **133**, 14236. (b) J. D. Rinehart, M. Fang, W. J. Evans, J. R. Long, *Nat. Chem.*, 2011, **3**, 538; (c) M. Urdampilleta, S. Klyatskaya, J. P. Cleuziou, M. Ruben and W. Wernsdorfer, *Nat. Mater.*, 2011, **10**, 502; (d) L. Bogani and W. Wernsdorfer, *Nat. Mater.*, 2008, **7**, 179.

7. (a) A. Ardavan and S. J. Blundell, *J. Mater. Chem.*, 2009, **19**, 1754. (b) F. Troiani and M. Affronte, *Chem. Soc. Rev.*, 2011, **40**, 3119; (c) P. C. E. Stamp and A. Gaita-Ariño, *J. Mater. Chem.*, 2009, **19**, 1718; (d) J. Lehmann, A. Gaita-Ariño, E. Coronado and D. Loss, *Nat. Nanotechnol.*, 2007, **2**, 312; (e) M. N. Leuenberger and D. Loss, *Nature*, 2001, **410**, 789.

8. (a) R. Sessoli, L. Hui, A. R. Schake, S. Wang, J. B. Vincent, K. Folting, D. Gatteschi and G. Christou, *J. Am. Chem. Soc.* 1993, **115**, 1804; (b) R. Sessoli, D. Gatteschi, A. Caneschi and M. A. Novak, *Nature*, 1993, **365**, 141; (c) J.-P. Zhao, B. W. Hu, X. F. Zhang, Q. Yang, M. S. El Fallah, J. Ribas, and X. H. Bu, *Inorg. Chem.* 2010, **49**, 11325.

9. (a) D. W. Boukhvalov, V. V. Dobrovitski, P. Kögerler, M. Al-Saqer, M. I. Katsnelson, A. I. Lichtenstein and B. N. Harmon, *Inorg. Chem.*, 2010, **49**, 10902; (b) T. Glaser, *Chem. Commun.* 2011, **47**, 116; (c) A. Grigoropoulos, M. Pissas, P. Papatolis, V. Psycharis, P. Kyritsis and Y. Sanakis, *Inorg. Chem.*, 2013, **52**, 12869; (d) A. K. Boudalis, M. Pissas, C. P. Raptopoulou, V. Psycharis, B. Abarca and R. Ballesteros, *Inorg. Chem.*, 2008, **47**, 10674. (e) G. Lazari, T. C. S.,

C. P. Raptopoulou, V. Psycharis, M. Pissas, S. P. Perlepes and A. K. Boudalis, *Dalton Trans.*, 2009, 3215; (f) M. Shanmugam, S. Vaidya, A. Upadhyay, S. K. Singh, T. Gupta, S. Tewary, S. Langley, J. Walsh, K. S. Murray and G. Rajaraman, *Chem. Commun.*, DOI: 10.1039/C4CC08305A,

10. (a) S. Osa, T. Kido, N. Matsumoto, N. Re, A. Pochaba, J. Mrozinski, *J. Am. Chem. Soc.*, 2004, **126**, 420; (b) C. M. Zaleski, E. C. Depperman, J. W. Kampf, M. L. Kirk, V. L Pecoraro, *Angew Chem., Int Ed.*, 2004, **43**, 3912; (c) T. K. Prasad, M. V. Rajasekharan and J. P. Costes, *Angew Chem., Int. Ed.*, 2007, **46**, 2851; (d) G. P. Guedes, S. Soriano, L. A. Mercante, N. L. Speziali, M. A. Novak, M. Andruh and M. G. F. Vaz., *Inorg. Chem.*, 2013, **52**, 8309; (e) J. Ruiz, G. Lorusso, M. Evangelisti, E. K. Brechin, S. J. A. Pope and E. Colacio, *Inorg. Chem.*, 2014, **53**, 3586; (f) M. A. Palacios, S. T.-Padilla, J. Ruiz, J. M. Herrera, S. J. A. Pope, E. K. Brechin and E. Colacio, *Inorg. Chem.*, 2014, **53**, 1465; (g) A. Upadhyay, S. K. Singh, C. Das, R. Mondol, S. K. Langley, K. S. Murray, G. Rajaraman and M. Shanmugam, *Chem. Commun.*, 2014, **50**, 8838; (h) Y. F. Zeng, G. C. Xu, X. Hu, Z. Chen, X. H. Bu, S. Gao, and E. C. Sañudo, *Inorg. Chem.*, 2010, **49**, 9734; (i) S.-D. Han, S. -J. Liu, Q. -L. Wang, X. -H. Miao, T. -L. Hu and X. -H. Bu, *Cryst. Growth Des.*, 2015, **15**, 2253; (j) S.-J. Liu, Y. -F. Zeng, L. Xue, S. -D. Han, J. -M. Jia, T. -L. Hu and X. H. Bu, *Inorg. Chem. Front.*, 2014, **1**, 200.

11. (a) R. J. Blagg, L. Ungur, F. Tuna, J. Speak, P. Comar, D. Collison, W. Wernsdorfer, E. J. L. McInnes, L. F Chibotaru and R. E. P Winpenny. *Nature Chem.*, 2013, **5**, 673; (b) R. J. Blagg, C. A. Muryn, E. J. L McInnes, F. Tuna and R. E. P. Winpenny, *Angew. Chem., Int. Ed.*, 2011, **50**, 6530.

12. (a) E. Lucaccini, L. Sorace, M. Perfetti, J. -P. Costes and R. Sessoli, *Chem. Commun.*, 2014, **50**, 1648; (b) F. Gao, L. Cui, Y. Song, Y. -Z. Li, J. -L. Zuo, *Inorg. Chem.*, 2014, **53**, 562; (c) J. J.

Baldoví, S. C. Serra, J. M. Clemente-Juan, E. Coronado, A. G. Arin and A. Palií, *Inorg. Chem.*, 2012, **51**, 12565; (d) G. Rajaraman, S. K. Singh, T. Gupta and M. Shanmugam *Chem. Commun.*, DOI: 10.1039/C4CC05522E

13. (a) P.-H. Lin, T. J. Burchell, R. Clerac and M. Murugesu, *Angew. Chem., Int. Ed.*, 2008, **47**, 8848; (b) G.-F. Xu, Q.-L. Wang, P. Gamez, Y. Ma, R. Clerac, J. Tang, S.-P. Yan and P. Cheng, D.-Z. Liao, *Chem. Commun.*, 2010, **46**, 1506; (c) K. A. Thiakou, V. Bekiari, C. P. Raptopoulou, V. Psycharis, P. Lianos and S. P. Perlepes, *Polyhedron*, 2006, **25**, 2869; (d) S.-S. Bao, L.-F. Ma, Y. Wang, L. Fang, C.-J. Zhu, Y.-Z. Li, L.-M. Zheng, *Chem.—Eur. J.* 2007, **13**, 2333; (e) S. J. Liu, J.-P. Zhao, W.-C. Song, S.-D. Han, Z.-Y. Liu and X.-H. Bu, *Inorg. Chem.*, 2013, **52**, 2103.

14. (a) I. J. Hewitt, Y. Lan, C. E. Anson, J. Luzon, R. Sessoli and A. K. Powell, *Chem. Commun.*, 2009, 6765; (b) J. Tang, I. J. Hewitt, T. N. Madhu, G. Chastanet, W. Wernsdorfer, C. E. Anson and A. K. Powell, *Angew. Chem., Int. Ed.*, 2006, **45**, 1729; (c) M. U. Anwar, S. S. Tandon, L. N. Dawe, F. Habib, M. Murugesu and L. K. Thompson, *Inorg. Chem.* 2012, **51**, 1028.

15. (a) B.-Q. Ma, D.-S. Zhang, S. Gao, T.-Z. Jin, C.-H. Yan, G.-X. Xu, *Angew. Chem., Int. Ed.*, 2000, **39**, 3644; (b) Y. Gao, G.-F. Xu, Z. L. hao, J. Tang and Z. Liu, *Inorg. Chem.*, 2009, **48**, 11495; (c) Y. Bi, X.-T. Wang, W. Liao, X. Wang, R. Deng, H. Zhang, S. Gao, *Inorg. Chem.*, 2009, **48**, 11743; (d) N. M. Randell, M. U. Anwar, M. W. Drover, L. N. Dawe and L. K. Thompson, *Inorg. Chem.*, 2013, **52**, 6731; (e) S.-D. Han, X. -H. Miao, S.-J. Liu and X.-H. Bu, *Inorg. Chem. Front.*, 2014, **1**, 549; (f) F. C. Liu, Y. -F. Zeng, J. -P. Zhao, B. W. Hu, X. Hu, J. Ribasc and X. H. Bu, *Dalton Trans.*, 2009, 2074.

16. (a) R. J. Blagg, C. A. Muryn, E. J. L. McInnes, F. Tuna and R. E. P. Winpenny, *Angew. Chem. Int. Ed.*, 2011, **50**, 6530; (b) D. T. Thielemann, A. T. Wagner, Y. Lan, C. E. Anson, M. T.

- Gamer, A. K. Powell and P. W. Roesky, *Dalton Trans.*, 2013, **42**, 14794; (c) M. T. Gamer, Y. Lan, P. W. Roesky, A. K. Powell and R. Cle'rac, *Inorg.Chem.*, 2008, **47**, 6581; (d) J.-B. Peng, X.-J. Kong, Y.-P. Ren, L.-S. Long, R.-B. Huang and L.-S. Zheng, *Inorg. Chem.*, 2012, **51**, 2186; (e) H. Tian, L. Zhao, H. Lin, J. Tang and G. Li *Chem. Eur. J.* 2013, **19**, 13235.
17. (a) D.-S. Zhang, B.-Q. Ma, T.-Z. Jin, S. Gao, C.-H. Yan and T. C. W Mak, *New J. Chem.*, 2000, **24**, 61; (b) N. Mahe, O. Guillou, C. Daiguebonne, Y. G\_erault, A. Caneschi, C. Sangregorio, C J. Y. hane-Ching, P. E. Car and T. Roisnel, *Inorg. Chem.*, 2005, **44**, 7743; (c) B. Hussain, D. Savard, T. J. Burchell, W. Wernsdorfer and M. Murugesu, *Chem. Commun.*, 2009, 1100; (d) S. Xue, L. Zhao, Y. N. Guo, P. Zhang and J. K. Tang, *Chem. Commun.*, 2012, **48**, 8946; (e) L. Ungur, S. K. Langley, T. N. Hooper, B. Moubaraki, E. K. Brechin, K. S. Murray and L. F. Chibotaru, *J. Am. Chem. Soc.*, 2012, **134**, 18554.
18. X. -J. Zheng, L.-P. Jin and S. Gao, *Inorg. Chem.* 2004, **43**, 1600.
19. (a) T. Kajiwara, H. Wu, T. Ito, N. Iki and S. Miyano, *Angew. Chem., Int. Ed.*, 2004, **43**, 1832. (b) V. Chandrasekhar, P. Bag and E. Colacio, *Inorg. Chem.*, 2013, **52**, 4562–4570.
20. (a) G. Xu, Z.-M. Wang, Z. He, Z. Lü, C.-S. Liao and C.-H. Yan, *Inorg. Chem.*, 2002, **41**, 6802; (b) G.-F. Xu, P. Gamez, S. J. Teat and J. Tang, *Dalton Trans.* 2010, **39**, 4353.
21. (a) K. Manseki and S. Yanagida, *Chem. Commun.*, 2007, 1242; (b) L. G. Westin, M. Kritikos, A. Caneschi, *Chem Commun.*, 2003, 1012; (c) X. Yang, R. A. Jones and M. J. Wiester, *Dalton Trans.*, 2004, 1787; (d) A. Kornienko, T. J. Emge, G. A. Kumar, R. E. Riman and J. G. Brennan, *J. Am. Chem. Soc.*, 2005, **127**, 3501.
22. (a) P. C. Andrews, T. Beck, C. M. Forsyth, B. H. Fraser, P. C. Junk, M. Massi and P. W. Roesky *Dalton Trans.*; **2007**, 5651; (b) R. Wang, H. D. Selby, H. Liu, M. D. Carducci, T. Jin, Z. Zheng, J. W. Anthis and R. J. Staples, *Inorg. Chem.*, 2002, **41**, 278.

23. (a) V. Chandrasekhar, B. M. Pandian, R. Azhakar, J. J. Vittal and R. Clérac, *Inorg. Chem.*, 2007, **46**, 5140; (b) V. Chandrasekhar, B. M. Pandian, R. Boomishankar, A. Steiner, J. J. Vittal, A. Hourri and R. Clérac, *Inorg. Chem.*, 2008, **47**, 4918; (c) V. Chandrasekhar, P. Bag, W. Kroener, K. Gieb and P. Müller, *Inorg. Chem.*, 2013, **52**, 13078; (d) V. Chandrasekhar, S. Das, A. Dey, S. Hossain, F. Lloret and E. Pardo, *Eur. J. Inorg. Chem.*, 2013, 4506. (e) V. Chandrasekhar, S. Das, A. Dey, S. Hossain, S. Kundu, and E. Colacio, *Eur. J. Inorg. Chem.*, 2014, 397; (f) C. Meseguer, S. T.-Padilla, M. M. Hänninen, R. Navarrete, A. J. Mota, M. Evangelisti, J. Ruiz and E. Colacio, *Inorg. Chem.*, DOI: dx.doi.org/10.1021/ic501915j (g) A. Deb, T. T. Boron, M. Itou, Y. Sakurai, T. Mallah, V. L. Pecoraro and J. E. Penner-Hahn, *J. Am. Chem. Soc.*, 2014, **136**, 4889; (h) C. M. Zaleski, J. W. Kampf, T. Mallah, M. L. Kirk and V. L. Pecoraro, *Inorg. Chem.*, 2007, **46**, 1954; (i) J. Goura, R. Guillaume, E. Rivière and V. Chandrasekhar, *Inorg. Chem.*, 2014, **53**, 7815; (j) P. Bag, A. Chakraborty, G. Rogez and V. Chandrasekhar, *Inorg. Chem.*, 2014, **53**, 6524.
24. (a) S. Das, S. Hossain, A. Dey, S. Biswas, J.-P. Sutter and V. Chandrasekhar, *Inorg. Chem.*, 2014, **53**, 5020–5028; (b) V. Chandrasekhar, P. Bag and E. Colacio, *Inorg. Chem.*, 2013, **52**, 4562; (c) S. Das, S. Hossain, A. Dey, S. Biswas, J.-P. Sutter and V. Chandrasekhar, *Inorg. Chem.*, 2014, **53**, 5020–5028; (d) T. Fukuda, N. Shigeyoshi, T. Yamamura and N. Ishikawa, *Inorg. Chem.*, 2014, **53**, 9080; (e) J. J. Le Roy, L. Ungur, I. Korobkov, L. F. Chibotaru and M. Murugesu, *J. Am. Chem. Soc.*, 2014, **136**, 8003; (f) F. Habib, G. Brunet, V. Vieru, I. Korobkov, L. F. Chibotaru and M. Murugesu, *J. Am. Chem. Soc.*, 2013, **135**, 13242; (g) V. E. Campbell, H. Bolvin, E. Rivière, R. Guillot, W. Wernsdorfer and T. Mallah, *Inorg. Chem.*, 2014, **53**, 2598.
25. V. Chandrasekhar, S. Hossain, S. Das, S. Biswas and J.-P. Sutter, *Inorg. Chem.*, 2013, **52**, 6346.

26. S. Das, A. Dey, S. Biswas, E. Colacio and V. Chandrasekhar, *Inorg. Chem.*, 2014, **53**, 3417.
27. (a) H. Lueken, *Magnetochemie*, Teubner, Stuttgart, Germany, 1999; (b) 28. M. Speldrich, H. Schilder, H. Lueken and P. Kögerler, *Isr. J. Chem.* 2011, **51**, 215–227; (c) J. van Leusen, M. Speldrich, H. Schilder, P. Kögerler, *Coord. Chem. Rev.* 2015, **289–290**, 137–148.
28. Cole, K.S.; Cole, R.H. *J. Chem. Phys.* 1941, **9**, 341–351.
29. (a) Vogel's Textbook of Practical Organic Chemistry, 5th ed.; B. S. Furniss, A. J. Hannaford, P. W. G. Smith, A. R. Tatchell, Eds. ELBS and Longman: London, **1989**. (b) D. B. G. Williams and M. Lawton, *J. Org. Chem.* 2010, **75**, 8351–8354. (c) X. Zeng, D. Coquiére, A. Alenda, E. Garrier, T. Prangé, Y. Li, O. Reinaud and I. Jabin, *Chem.—Eur. J.* 2006, **12**, 6393–6402.
30. (a) *SMART & SAINT Software Reference manuals*, Version 6.45; Bruker Analytical X-ray Systems, Inc.: Madison, WI, **2003**. (b) G. M. Sheldrick, *SADABS, a software for empirical absorption correction*, Ver. 2.05; University of Göttingen: Göttingen, Germany, 2002. (c) *SHELXTL Reference Manual*, Ver. 6.1; Bruker Analytical X-ray Systems, Inc.: Madison, WI, **2000**. (d) G. M. Sheldrick, *SHELXTL*, Ver. 6.12; Bruker AXS Inc.: Madison, WI, 2001. (e) G. M. Sheldrick, *SHELXL97, Program for Crystal Structure Refinement*; University of Göttingen: Göttingen, Germany, 1997. (f) P. Van der Sluis and A. L. Spek, *Acta Crystallogr., Sect. A: Found. Crystallogr.* **1990**, **46**, 194. (g) A. L. Spek, *Acta Crystallogr., Sect. A: Found. Crystallogr.* 1990, **46**, c34. (h) K. Bradenburg, *Diamond, Ver. 3.1eM*; Crystal Impact GbR: Bonn, Germany, **2005**.



## Graphical Abstract

## Pentanuclear [2.2] Spirocyclic Lanthanide(III) Complexes: Slow Magnetic Relaxation of the Dy<sup>III</sup> Analogue

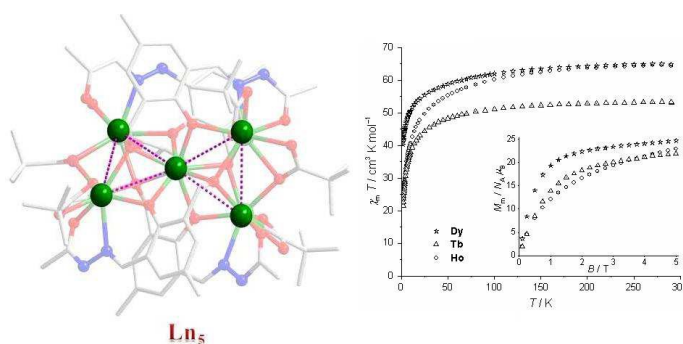
Sourav Biswas,<sup>a</sup> Sourav Das,<sup>a</sup> Jan van Leusen,<sup>b</sup> Paul Kögerler<sup>\*b</sup> and Vadapalli Chandrasekhar<sup>\*a,c</sup>

<sup>a</sup> Department of Chemistry, Indian Institute of Technology Kanpur, Kanpur-208016, India.

<sup>b</sup> Institut für Anorganische Chemie, RWTH Aachen University, D-52074 Aachen, Germany.

<sup>c</sup> National Institute of Science Education and Research, Institute of Physics Campus,

Sachivalaya Marg, PO: Sainik School, Bhubaneswar - 751 005, India.



The reaction of multisite coordinating Schiff base ligand (LH<sub>3</sub>) with LnCl<sub>3</sub>·6H<sub>2</sub>O in presence of triethyl amine afforded homometallic pentanuclear compounds, [Ln<sub>5</sub>(LH)<sub>4</sub>(η<sup>1</sup>-Piv)(η<sup>2</sup>-Piv)<sub>3</sub>(μ<sub>2</sub>-η<sup>2</sup>η<sup>1</sup>Piv)<sub>2</sub>(H<sub>2</sub>O)]·Cl (Ln = Dy<sup>III</sup>, Tb<sup>III</sup> and Ho<sup>III</sup>) possessing a [2.2] spirocyclic topology. Detailed magnetic studies reveal that the Dy<sup>III</sup> analogue exhibited slow relaxation of magnetization in the presence of a 3000 G dc field.